

# Brief Communication: Recent estimates of glacier mass loss for western North America from laser altimetry

Brian Menounos<sup>1,2\*</sup>, Alex Gardner<sup>3</sup>, Caitlyn Forentine<sup>4</sup>, Andrew Fountain<sup>5</sup>

<sup>1</sup>University of Northern British Columbia, Geography Earth and Environmental Sciences, Prince George BC, V2N 4Z9, Canada

<sup>2</sup>Hakai Institute, Campbell River, BC, Canada

<sup>3</sup>Jet Propulsion Laboratory, California Institute of Technology, Pasadena, CA 91109, USA

<sup>4</sup>United States Geological Survey Northern Rocky Mountain Science Center, Bozeman, MT, USA

<sup>5</sup>Portland State University, Department of Geology, Portland, OR, 97201, USA

\*Corresponding author: [menounos@unbc.ca](mailto:menounos@unbc.ca)

*Correspondence to:* Brian Menounos ([menounos@unbc.ca](mailto:menounos@unbc.ca))

**Abstract.** Glaciers in Western North American outside of Alaska are often overlooked in global studies, because their potential to contribute to changes in sea level is small. Nonetheless, these glaciers represent important sources of freshwater, especially during times of drought. Differencing recent ICESat-2 data from a digital elevation model derived from a combination of synthetic aperture radar data (TerraSAR-X/TanDEM-X), we find that over the period 2013-2021, glaciers in western North America lost mass at a rate of  $-12.3 \pm 3.5$  Gt yr<sup>-1</sup>. This rate is comparable to the rate of mass loss ( $-11.7 \pm 1.0$  Gt yr<sup>-1</sup>) for the period 2018-2022 calculated through trend analysis using ICESat-2 and Global Ecosystems Dynamics Investigation (GEDI) data.

## 1 Introduction

Western North American glaciers outside of Alaska cover 14,384 km<sup>2</sup> of mountainous terrain (Pfeffer et al. 2014). Although the global sea level equivalent of these glaciers is only  $2.6 \pm 0.7$  mm (Farinotti et al., 2019), these glaciers provide important thermal buffering capacity during late summer or during times of drought (Moore et al., 2009). Early attempts to define regional estimates of glacier mass change suffered from sparse, in-situ glaciological observations, non-uniform distribution of geodetic measurements, and uncertainties in gravimetric assessments due to changes in seasonal water storage (Jacob et al., 2012;



28 Gardner et al., 2013; Zemp et al., 2019). Two recent studies combined publicly-available geodetic datasets and statistical  
29 methods to yield mass change estimates with much less spatial bias and lower overall uncertainties (Menounos et al., 2019;  
30 Hugonnet et al., 2021). Both of these studies rely on DEMs generated from NASA's Advanced Spaceborne Thermal Emission  
31 and Reflection Radiometer (ASTER) sensor aboard the Terra satellite. Unfortunately, Terra's orbit is degrading and will reach  
32 its end of life within the next 3-4 years. Additional datasets are thus required to quantify glacier mass loss in mountain  
33 environments where glacier loss is accelerating (Hugonnet et al., 2021), but recent studies leveraging laser altimetry in global  
34 glacier assessments have excluded glaciers in western North America (Jakob and Gourmelen, 2023). Here we provide new  
35 estimates of recent glacier mass loss based on laser altimetry data for the western United States and Canada which is Region  
36 02 of the Randolph Glacier Inventory (Pfeffer et al., 2014).

## 37 **2 Data and methods**

### 38 **2.1 Altimetric data (ICESat-2 and GEDI)**

39 Altimetric data include observations made by NASA's Advanced Topographic Laser Altimeter System (ATLAS), which is a  
40 532 nm photon-counting laser system aboard the ICESat-2 satellite that operates between 88° N/S (Markus et al., 2017,  
41 Markus et al., 2017, Smith et al., 2021 ). We use version 5 of the ATL06 (land-ice surface heights) dataset that includes laser  
42 shots from 13 October 2018 to 12 October, 2022. We also used Global Ecosystem Dynamics Investigation (GEDI) laser data  
43 (Liu et al., 2021, Dubayah et al. 2021) acquired between 1 January, 2018 and 1 January, 2022 (GEDI02\_A release 2). GEDI  
44 is a 1064 nm, full-waveform laser that, because of its operation aboard the International Space Station, operates between 51.6°  
45 N/S.

### 46 **2.2 Digital elevation model**

47 The mass change estimate for approximately the last decade (2013 to 2020), herein referred to as the decadal estimate, uses  
48 the global, 30 m Copernicus DEM elevation data derived from the TanDEM-X Synthetic Aperture Radar (SAR) mission  
49 (Rizzoli et al., 2017) and made publicly available as the Glo30 product, herein referred to as COP-30 (European Space Agency,  
50 2023). Acquisition of the data used in COP-30 DEM occurred between 2010 and early 2015 and coverage represented about  
51 five individual SAR tiles in our study region. Because no gridded acquisition date exist for COP-30, we use an acquisition date  
52 of 2013, which coincides with the midpoint for the majority of DEM acquisitions (Rizzoli et al., 2017). As described below,  
53 we use the ambiguity of DEM acquisition dates as one source of uncertainty in our mass change estimate.

54  
55 For each subregion, we reprojected the COP-30 into the local UTM zone. The COP-30 vertical datum is EGM96 which we  
56 converted to match the vertical datum of ICESat-2 (WGS84). ICESat-2 data for a given acquisition date were clipped to a



57 region of interest and the closest elevation of the COP-30 was extracted for a given laser shot. Elevation of both COP-30 and  
58 ICESat-2 were retained, as was the derived elevation change [m], rates of elevation change [m yr<sup>-1</sup>]. Other original attributes  
59 present with the ICESat-2 data (e.g. track number, effective laser shot radius, slope) were retained to maintain metadata  
60 continuity. Elevation change values that exceeded -20 or 20 m yr<sup>-1</sup> were excluded from subsequent analysis as it was assumed  
61 that these signals exceed the range of what is physically attributable to glacier processes.

62  
63 For the decadal estimate of mass change, each glacier polygon (RGI-6.0) within the study region was buffered by 1 km and  
64 then masked from the original glacier polygon, to capture areas adjacent to glaciers that we considered to be areas of stable  
65 terrain. Due to the buffer, we expect results to be robust to glacier polygon updates. Note that the recently released RGI-7.0  
66 has no changes from RGI-6.0 in our study area. Inspection of elevation change over stable terrain for all ICESat-2 laser shots  
67 ( $2.24 \times 10^6$ ) reveals a positive bias for almost every subregion, typically on the order of 0.1-0.5 m yr<sup>-1</sup> (ICESat-2 minus COP-  
68 30); this bias, however, did not substantially vary with elevation for a given region. Visual inspection of elevation change maps  
69 and review of acquisition dates of ICESat-2 data suggests this positive bias arises by laser shots over snow-covered terrain  
70 (Enderlin et al., 2022). We therefore limit our analysis to the ablation season when the positive bias associated with snow-  
71 covered terrain is minimized. Confirmation of the source of this bias is revealed when the analysis of rates of elevation change  
72 is limited to ICESat-2 laser shots acquired between 1 August and 1 October. For these late summer laser shots, we respectively  
73 observe a mean bias and uncertainty ( $\pm 1$  sigma) over stable terrain of 0.038 and 1.53 m yr<sup>-1</sup>.

### 74 **2.3 Recent rate of elevation change from ICESat-2 and GEDI**

75 For the period 2018-2022, herein referred to as the recent period, we first create altimetry anomalies by differencing ICESat-  
76 2 and GEDI laser shots to the COP-30 DEM. A least squares regression that includes an offset, trend and seasonal sinusoidal  
77 terms is fit to anomalies within a 250 m radius search window. The y-intercept of the regression is set to the year 2020. We  
78 exclude any ICESat-2 or GEDI laser shots if they deviate more than 250 m from the COP-30 DEM, or if they deviate by more  
79 than 150 m from the median anomaly within the 250 m search radius. The search radius and median anomaly threshold were  
80 selected to omit elevation change signals that were not physically realistic. Regression fits were excluded from further analysis  
81 if: (i) there were fewer than five data points for given search window; (ii) the temporal span of observations is less than three  
82 years; (iii) the root mean squared error (RMSE) of the fit residuals exceed 5.0 m yr<sup>-1</sup> and (iv); the seasonal amplitude of the  
83 least squares fit exceeds 10 m yr<sup>-1</sup>. This did not disrupt the representation of glacier hypsometry, i.e. results were well  
84 distributed across glacierized elevations in the study region. We use the trend obtained from the regression to the 250 m radius  
85 to represent elevation change.

86

### 87 **2.4 Mass change uncertainty**



88 Uncertainty in mass change originates from errors in rates of elevation change and volume-to-mass conversion factor. We use  
89  $850 \text{ kg m}^{-3}$  and its associated uncertainty term ( $\pm 60 \text{ kg m}^{-3}$ ) for mass conversion (Huss, 2013). We generate bootstrapped errors  
90 in total volume change using a Monte Carlo method (Chernick et al. 2011). We first temporally randomize the laser altimetric  
91 data, randomly choose the acquisition date of the COP-30 DEM (2012, 2013, 2014) and sample 5% of the data with  
92 replacement 10,000 times. Total volume change over glacierized terrain is calculated for each synthetic dataset by multiplying  
93 the rate of elevation change by the area of glaciers within a given elevation bin (100 m bins). We then take 5% and 95%  
94 modelled volume change as our uncertainty.

95  
96 Error in mass change is then calculated from:

$$97 \sqrt{(dV_{\sigma} \cdot \rho)^2 + (\rho_{\sigma} \cdot dV)^2} \quad (1)$$

98  
99  
00 Where  $dV_{\sigma}$  is the uncertainty of volume change generated from the Monte Carlo method,  $\rho$  is material density ( $850 \text{ kg m}^{-3}$ ),  
01  $\rho_{\sigma}$  is uncertainty of density ( $60 \text{ kg m}^{-3}$ ) and  $dV$  is the change in volume.

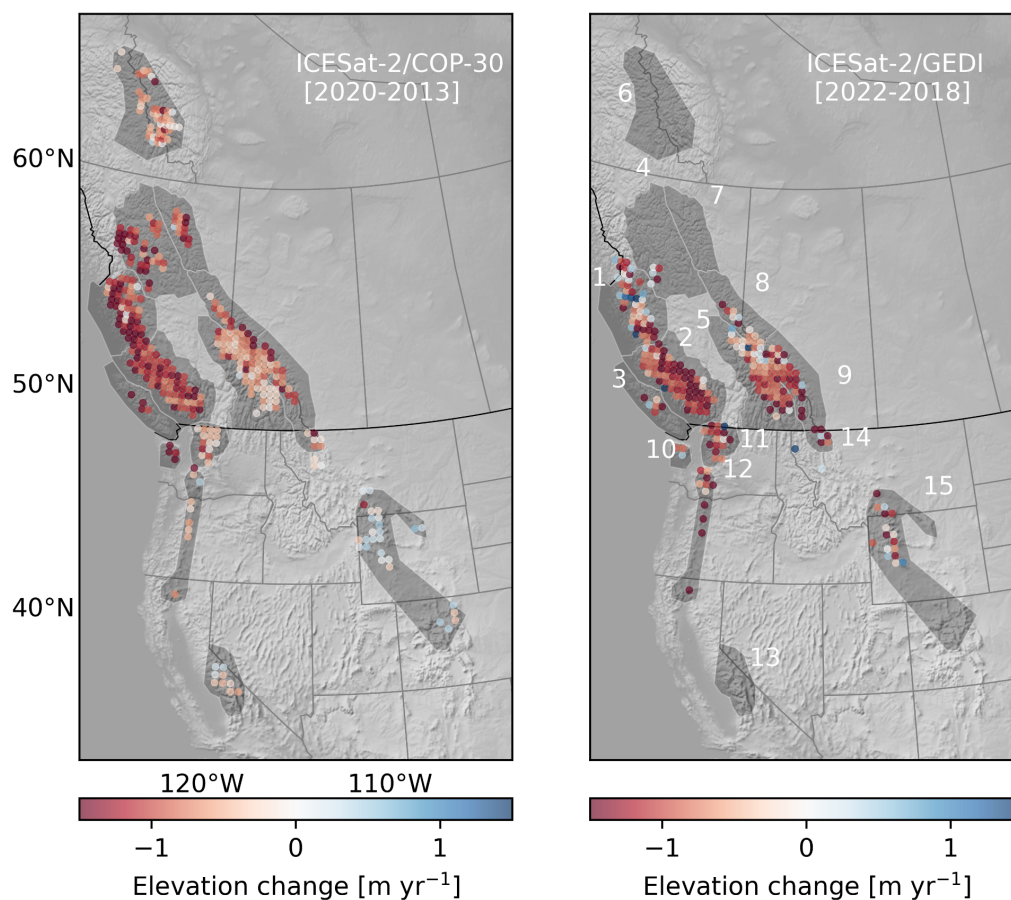
### 02 **3.0 Results**

03 To minimize the impact of the seasonal snow signal, we limit our analysis of mass change using ICESat-2 and COP-30  
04 elevation changes to ICESat-2 data acquired during the latter half of the ablation season (1 August - 1 October). Glaciers  
05 throughout the western United States and Canada thinned both during the decadal and recent period with prominent thinning  
06 within the Southern Coast Mountains, a region that contains nearly one half of the total ice cover of the study region (Fig. 1.  
07 For the period 2013-2021 (median date of ICESat-2 data is 26 August, 2020), we estimate a rate of mass change of  $-12.3 \pm 3.5$   
08  $\text{Gt yr}^{-1}$  (Fig. 1). This measurement agrees within the rate of mass change [ $-12.3 \pm 4.6 \text{ Gt yr}^{-1}$ ] reported for the period 2009–  
09 2018 (Menounos et al., 2019) and the estimate [ $-12.3 \pm 3.0 \text{ Gt yr}^{-1}$ ] for the period 2015-2019 based primarily on ASTER data  
10 (Hugonnet et al., 2021). Comparable estimates of mass loss exist for western North America for the period 1961-2016 [ $-12 \pm$   
11  $6 \text{ Gt yr}^{-1}$ ] and for the period 2002-2009 [ $-14 \pm 3 \text{ Gt yr}^{-1}$ ] respectively from Zemp et al., (2019) and Gardner et al., (2013).  
12 Figure 2 shows results using only ICESat-2 and GEDI laser shots and rates of elevation change determined through least  
13 squares fitting (i.e. the recent period), glaciers lost  $-11.7 \pm 1.0 \text{ Gt yr}^{-1}$  of mass for the period 2018-2022 (Fig. 2). Mass change  
14 rates per subregions (Fig. 1) are summarized elsewhere (SM Table 1). The effect of small sample size is evident in the larger  
15 uncertainty of elevation change at highest and lowest elevations, but the contribution of this error to total mass change is small  
16 since little total glacierized area exists at these elevations.



#### 17 **4.0 Discussion and Conclusion**

18 Our geodetic balance obtained from laser altimetry using least squares fitting provides the most recent mass change update for  
19 western North America, a region excluded in a recent global assessment of glacier mass loss using laser altimetry from  
20 CryoSat-2 data (Jakob and Gourmelen, 2023). While our trend analysis provides a robust estimate of recent glacier mass  
21 change, insufficient sampling precludes our assessment of mass loss for regions where laser altimetry data are sparse. This  
22 sparseness is especially pronounced in regions north of GEDI data coverage ( $51.6^{\circ}$  N) and regions characterised by small  
23 glaciers (Fig. 2). Our decadal estimates of glacier mass loss provide more insight into sub-regional patterns of glacier mass  
24 loss, but insight is offset by the additional uncertainty of radar penetration at highest elevation and the ambiguity of the  
25 acquisition data for the COP-30 DEM. Others report penetration of the Tandem-X radar signal into high elevation firn and  
26 snow surfaces (Abdullahi et al., 2019). The potential of this penetration bias to greatly affect our results is limited since it is  
27 spatially limited to elevation zones that typically represent  $< 1\text{-}2\%$  of the total areas within a given region, based on the  
28 elevation distribution of glaciers in the western United States and Canada and assumptions of the associated distribution of  
29 firn and/or snow.



30

31 **Figure 1: Elevation change [m yr<sup>-1</sup>] for western North American glaciers. Data aggregated to points with 50 km spacing. Left panel:**  
32 **Elevation change [m yr<sup>-1</sup>] determined from ICESat-2 and COP-30 data (2022 - 2013); Right Panel: Elevation change [m yr<sup>-1</sup>] from**  
33 **trend analysis over period 2022-2018 from ICESat-2 (Smith et al. 2021) and GEDI laser altimetric (Dubayah et al. 2021) data.**  
34 **Numbers refer to glacierized regions of Western North America (RGI region 02, Pfeffer et al. 2014). The regions include: (1) Central**  
35 **Coast (1,692 km<sup>2</sup>); (2) Southern Coast (7,181 km<sup>2</sup>); (3) Vancouver Island (15 km<sup>2</sup>); (4) Northern Interior (572 km<sup>2</sup>); (5) Southern**  
36 **Interior (1,959 km<sup>2</sup>); (6) Nahanni (657 km<sup>2</sup>); (7) Northern Rocky Mountains (415 km<sup>2</sup>); (8) Central Rocky Mountains (422 km<sup>2</sup>); (9)**  
37 **Southern Rocky Mountains (1,350 km<sup>2</sup>).**

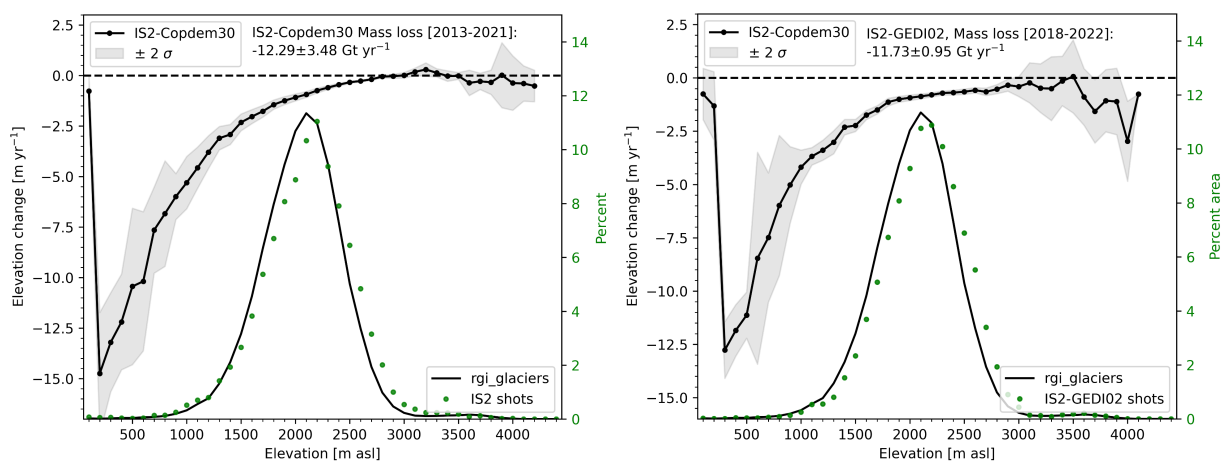
38

39 The regional pattern of elevation change obtained for the recent period shows areas of neutral or slight elevation gain (e.g.  
40 regions 1 and 5) that are not apparent in the map of decadal elevation change (Fig. 1). The most parsimonious explanation for  
41 these differences is the influence of spatially variable snow accumulation in these regions, though we cannot rule out the  
42 possibility of changing balance between ice dynamics and mass balance to explain the observed elevation changes. In addition,  
43 the decadal pattern largely accords with the notable zonal difference in elevation change observed by Menounos et al., (2019).  
44 A key finding of Hugonnet et al., (2021) was the notable accelerated mass loss in western North America during the period



45 2015-2019 relative to the start of the 21<sup>st</sup> century. Our recent and decadal estimates of glacier mass loss using independent  
 46 datasets confirms the magnitude of recent mass change for a comparably recent period (2018 to 2022), corroborating the  
 47 finding of accelerated mass loss from this previous study.

48  
 49  
 50



51  
 52

53 **Figure 2: Left Panel: Rates of elevation change [m yr<sup>-1</sup>] versus elevation for the period 2013-2021. Only laser shots from 1 August-**  
 54 **1 October (n=347,630) used in analysis. Light grey shading denotes uncertainty (5-95%) of elevation change. Black line and green**  
 55 **dots respectively indicate percent area of RGI ice and percentage of ICESat-2 laser shots within a given elevation bin. Right Panel:**  
 56 **Rates of elevation change [m yr<sup>-1</sup>] versus elevation for the period 2018-2022 from ICESat-2 and GEDI laser shots from least-squares**  
 57 **trend analysis (n=66,201). Light grey shading denotes uncertainty (5-95%) of elevation change. Black line and green dots respectively**  
 58 **indicate percent area of RGI ice and percentage of ICESat-2 (Smith et al. 2021) laser shots within a given elevation bin.**

59  
 60  
 61  
 62  
 63  
 64  
 65  
 66  
 67  
 68  
 69





70 **Code/Data availability**

71 Data reported in this paper is available upon request.

72

73 **Author Contribution**

74 Menounos proposed the study, completed the Copdem30 and ICESat-2 analysis and wrote the initial draft of the contribution  
75 and Gardner completed the ICESat-2 and GEDI analysis. All authors provided input, and commented on drafts of the  
76 manuscript.

77

78 **Acknowledgements**

79 The authors acknowledge constructive input from Rainey Aberle and Albin Wells which improved the quality and clarity of this manuscript.  
80 Any use of trade, firm, or product names is for descriptive purposes only and does not imply endorsement by the U.S. Government. This  
81 study was supported by the National Sciences and Engineering Research Council of Canada, the Tula Foundation, and the Canada Research  
82 Chairs Program.

83 **References**

84 Abdullahi, S., Wessel, B., Huber, M., Wendleder, A., Roth, A., and Kuenzer, C.: Estimating Penetration-Related  
85 X-Band InSAR Elevation Bias: A Study over the Greenland Ice Sheet, *Remote Sensing*, 11, 2903, 2019.

86 Chernick, M.R., González-Manteiga, W., Crujeiras, R.M., Barrios, E.B. (2011). Bootstrap Methods. In: Lovric,  
87 M. (eds) *International Encyclopedia of Statistical Science*. Springer, Berlin, Heidelberg.  
88 [https://doi.org/10.1007/978-3-642-04898-2\\_150](https://doi.org/10.1007/978-3-642-04898-2_150)

89 Dubayah, R., M. Hofton, J. Blair, J. Armston, H. Tang, S. Luthcke. GEDI L2A Elevation and Height Metrics  
90 Data Global Footprint Level V002. 2021, distributed by NASA EOSDIS Land Processes DAAC,  
91 [https://doi.org/10.5067/GEDI/GEDI02\\_A.002](https://doi.org/10.5067/GEDI/GEDI02_A.002). Accessed 2023-04-01.

92 Enderlin, E. M., Elkin, C. M., Gendreau, M., Marshall, H. P., O’Neel, S., McNeil, C., Florentine, C., and Sass,  
93 L.: Uncertainty of ICESat-2 ATL06- and ATL08-derived snow depths for glacierized and vegetated mountain  
94 regions, *Remote Sens. Environ.*, 283, 113307, 2022.

95 European Space Agency, 2023. Copernicus DEM – Global and European Digital Elevation Models.  
96 <https://doi.org/10.5270/ESA-c5d3d65>.

97 Farinotti, D., Huss, M., Fürst, J. J., Landmann, J., Machguth, H., Maussion, F., and Pandit, A.: A consensus  
98 estimate for the ice thickness distribution of all glaciers on Earth, *Nat. Geosci.*, 12, 168–173, 2019.

99 Gardner, A. S., Moholdt, G., Cogley, J. G., Wouters, B., Arendt, A. A., Wahr, J., Berthier, E., Hock, R., Pfeffer,  
:00 W. T., Kaser, G., Ligtenberg, S. R. M., Bolch, T., Sharp, M. J., Hagen, J. O., van den Broeke, M. R., and Paul, F.:  
:01 A reconciled estimate of glacier contributions to sea level rise: 2003 to 2009, *Science*, 340, 852–857, 2013.





- .02 Hugonnet, R., McNabb, R., Berthier, E., Menounos, B., Nuth, C., Girod, L., Farinotti, D., Huss, M., Dussailant,  
.03 I., Brun, F., and Käab, A.: Accelerated global glacier mass loss in the early twenty-first century, *Nature*, 592,  
.04 726–731, 2021.
- .05 Huss, M.: Density assumptions for converting geodetic glacier volume change to mass change, *The Cryosphere*,  
.06 7, 877–887, 2013.
- .07 Jacob, T., Wahr, J., Pfeffer, W. T., and Swenson, S.: Recent contributions of glaciers and ice caps to sea level  
.08 rise, *Nature*, 482, 514–518, 2012.
- .09 Jakob, L. and Gourmelen, N.: Glacier mass loss between 2010 and 2020 dominated by atmospheric forcing,  
.10 *Geophys. Res. Lett.*, 50, <https://doi.org/10.1029/2023gl102954>, 2023.
- .11 Liu, A., Cheng, X., and Chen, Z.: Performance evaluation of GEDI and ICESat-2 laser altimeter data for terrain  
.12 and canopy height retrievals, *Remote Sens. Environ.*, 264, 112571, 2021.
- .13 Markus, T., Neumann, T., Martino, A., Abdalati, W., Brunt, K., Csatho, B., Farrell, S., Fricker, H., Gardner, A.,  
.14 Harding, D., Jasinski, M., Kwok, R., Magruder, L., Lubin, D., Lutheke, S., Morison, J., Nelson, R.,  
.15 Neuenschwander, A., Palm, S., Popescu, S., Shum, C. K., Schutz, B. E., Smith, B., Yang, Y., and Zwally, J.: The  
.16 Ice, Cloud, and land Elevation Satellite-2 (ICESat-2): Science requirements, concept, and implementation,  
.17 *Remote Sens. Environ.*, 190, 260–273, 2017.
- .18 Menounos, B., Hugonnet, R., Shean, D., Gardner, A., Howat, I., Berthier, E., Pelto, B., Tennant, C., Shea, J.,  
.19 Noh, M.-J., Brun, F., and Dehecq, A.: Heterogeneous Changes in Western North American Glaciers Linked to  
.20 Decadal Variability in Zonal Wind Strength, *Geophys. Res. Lett.*, 46, 200–209, 2019.
- .21 Moore, R. D., Fleming, S. W., Menounos, B., Wheate, R., Fountain, A., Stahl, K., Holm, K., and Jakob, M.:  
.22 Glacier change in western North America: influences on hydrology, geomorphic hazards and water quality,  
.23 *Hydrol. Process.*, 23, 42–61, 2009.
- .24 Pfeffer, W. T., Arendt, A. A., Bliss, A., Bolch, T., Cogley, J. G., Gardner, A. S., Hagen, J.-O., Hock, R., Kaser,  
.25 G., Kienholz, C., and Others: The Randolph Glacier Inventory: a globally complete inventory of glaciers, *J.*  
.26 *Glaciol.*, 60, 537–552, 2014.
- .27 Rizzoli, P., Martone, M., Gonzalez, C., Wecklich, C., Borla Tridon, D., Bräutigam, B., Bachmann, M., Schulze,  
.28 D., Fritz, T., Huber, M., Wessel, B., Krieger, G., Zink, M., and Moreira, A.: Generation and performance  
.29 assessment of the global TanDEM-X digital elevation model, *ISPRS J. Photogramm. Remote Sens.*, 132, 119–  
.30 139, 2017.
- .31 Smith, B., S. Adusumilli, B. M. Csathó, D. Felikson, H. A. Fricker, A. Gardner, N. Holschuh, J. Lee, J. Nilsson,  
.32 F. S. Paolo, M. R. Siegfried, T. Sutterley, and the ICESat-2 Science Team. (2021). ATLAS/ICESat-2 L3A Land  
.33 Ice Height, Version 5 [Data Set]. Boulder, Colorado USA. NASA National Snow and Ice Data Center Distributed  
.34 Active Archive Center, <https://doi.org/10.5067/ATLAS/ATL06.005>. Date Accessed 10-16-2023.
- .35 Zemp, M., Huss, M., Thibert, E., Eckert, N., McNabb, R., Huber, J., Barandun, M., Machguth, H., Nussbaumer,  
.36 S. U., Gärtner-Roer, I., Thomson, L., Paul, F., Maussion, F., Kutuzov, S., and Cogley, J. G.: Global glacier mass  
.37 changes and their contributions to sea-level rise from 1961 to 2016, <https://doi.org/10.1038/s41586-019-1071-0>,



:38 2019.

:39